



Simulation model of direct torque control with discretized voltage vector intensities¹

Marko Rosić², Milan Bebić³, Nikola Đorđević³,
Miroslav Bjekić² and Marko Šućurović²

² Faculty of Technical Sciences Čačak, University of Kragujevac, Čačak, Serbia

³ School of Electrical Engineering, University of Belgrade, Belgrade, Serbia
e-mail marko.rosic@ftn.kg.ac.rs

Abstract: This paper describes the development process for direct torque control algorithm with multiple voltage vectors aiming to reduce torque ripple as a main drawback of DTC algorithm with discrete voltage vectors and switching tables. The idea and the selection principle of voltage vectors with different intensities that need to provide torque ripple reduction is given in Section 2. In Section 3, the developed Simulink model of the proposed DTC algorithm is described in detail and simulation results for different numbers of voltage vector intensities are shown. The model of proposed algorithm is convenient for students who attend the course of control of electric drives in order to comprehend DTC principle more easily. Experimental results of the proposed DTC method are presented in section 4, followed by the conclusion at the end of the paper.

Keywords: direct torque control, discretized voltage intensities, simulation, torque ripple reduction, EMF compensation.

1. INTRODUCTION

Direct torque control (DTC) from the moment of its appearing until today, suffered a number of modifications to eliminate its shortcomings of which the most important is a large torque ripple. In DTC algorithms that use discrete voltage vectors torque ripple can be reduced by applying voltage vectors with more intensities. A number of papers have been published so far concerning this topic. For instance, in [1],[2] the authors have presented DSVM-DTC algorithm which uses three basic voltage vectors in one switching cycle. In this way, it is possible to define a large number of resulting voltage vectors of different intensities and directions. By further increasing the number of voltage vectors, the switching table becomes more complicated and duration of the calculation cycle should be extended in order to prevent too high switching frequency (change of four or more voltage vectors in one cycle). For that reason DSVM-DTC method is limited in terms of ripple reduction because of the consequences brought by further increase of the available voltage vectors number. It can be said that the development of converters with higher voltage levels provided further existence

¹ This work was supported by grants (Projects No. TR33016 and TR33024) from the Ministry of Education, Science and Technological Development of Serbia

and development of algorithms that use DTC switching table especially when it comes to multilevel inverters and multi-phase drives [3],[4],[5]. Despite the simplicity of these algorithms excessive number of available voltage vectors can lead to problems in terms of the complexity of the switching table. Switching table for inverters with more than three voltage levels becomes very complex and therefore their application in practical implementations is rare. More complex structures of multi-level inverters also introduce challenges related to their configuration and control.

On the other side DVI-DTC algorithm (Discretized Voltage Intensities DTC) presented in [6] has been developed for standard two-level voltage source inverter. DVI-DTC algorithm retains the application of simple conventional switching table that defines the direction of one of the six basic voltage vectors. The intensity of the selected basic voltage vector is determined from the torque error according to the multilevel torque comparator. This enables decoupled selection of direction and the intensity of the voltage vector. The method offers easy upgrading, even automatic adaptation of algorithm and predefining of voltage vectors depending on the desired number of their intensities without changing the basic switching table. The main topic of this paper is the simulation model of DVI-DTC algorithm in *Matlab/Simulink*. The simulation is used prior to implementation on the real drive and helps students to better understand the principles of DTC. The basic DTC theory is described first and Simulink model of the proposed DVI-DTC algorithm is described in detail afterwards. At the end of the paper simulation and experimental results are shown confirming reduced torque ripple.

2. THEORY OF DIRECT TORQUE CONTROL WITH DISCRETIZED VOLTAGE VECTOR INTENSITIES

Conventional DTC algorithm [7] relies on the use of switching table (Table 1) that provides optimal choice between six basic active voltage vectors and two zero vectors (Fig. 1a) on the next switching period Δt .

Table 1. Switching table (selection of voltage direction)

S_ψ	S_m		
	1	0	-1
1	U_{i+1}	U_7 or U_8	U_{i-1}
-1	U_{i+2}	U_7 or U_8	U_{i-2}

DVI-DTC algorithm with multiple voltage intensities uses the same switching table (Table 1) to select the direction of the voltage vector depending on the flux and torque requirements (S_ψ and S_m) where i stands for number of sector ($i=1\dots 6$) where stator flux is located. The selection of voltage vector intensity that depends on the value of the torque error is provided by multilevel torque comparator.

Fig. 1a shows defined three intensities of the voltage vectors using PWM, whose selection depends on the value of the torque error. By involving higher number of voltage intensities, the torque ripple can be significantly reduced. The torque response is highly influenced by the intensity of the induced EMF, which leads to the steady state torque error depending on the motor speed. The influence of induced EMF on DVI-DTC algorithm was analyzed in detail in [8]. To eliminate the influence of induced EMF it is necessary to add the appropriate voltage (Fig. 1b) that should compensate its effect on torque error.

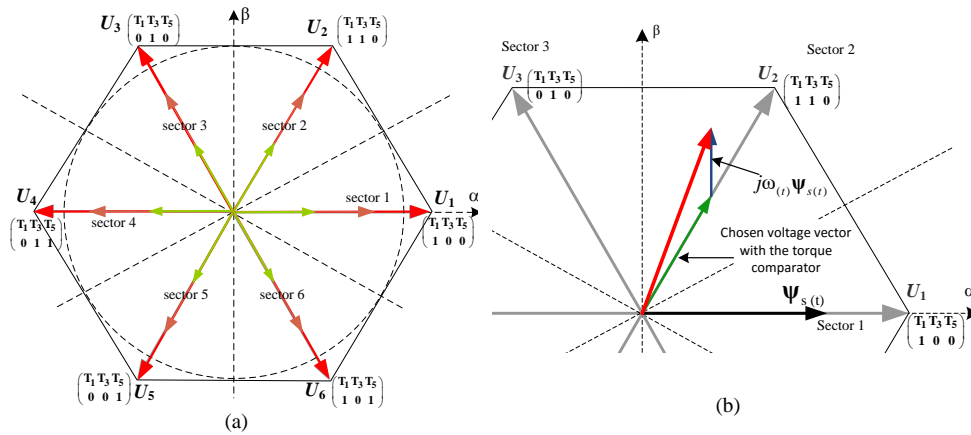


Figure 1. Defined discretized voltage intensities (a) and resulting voltage vector aiming to compensate EMF (b)

3. SIMULINK MODEL OF THE DVI-DTC ALGORITHM

Modeling and simulation of control algorithms is very important. Simulation allows us to test and examine developed algorithms before implementation in the real-time DSP systems [9]. Also, simulations are very useful in teaching the control of electric drives [10].

A simplified block scheme of the proposed DVI-DTC algorithm is presented in Fig. 2. As it has already been mentioned, selection of the voltage vector direction (two zero and six active vectors) is based on outputs of conventional flux and multilevel torque comparators. Selection of the voltage vector intensity is based on the value of torque error ΔT_e .

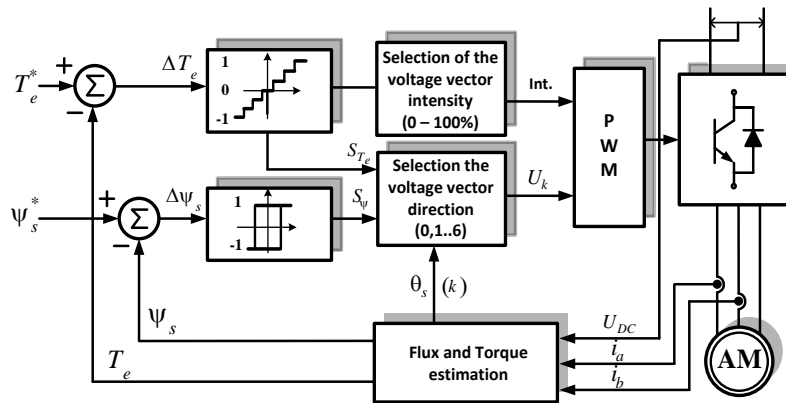


Figure 2. Block scheme of DVI-DTC algorithm

The simulation model of proposed DTC algorithm is made in *Matlab/Simulink* and the main window of the model is presented in Fig. 3.

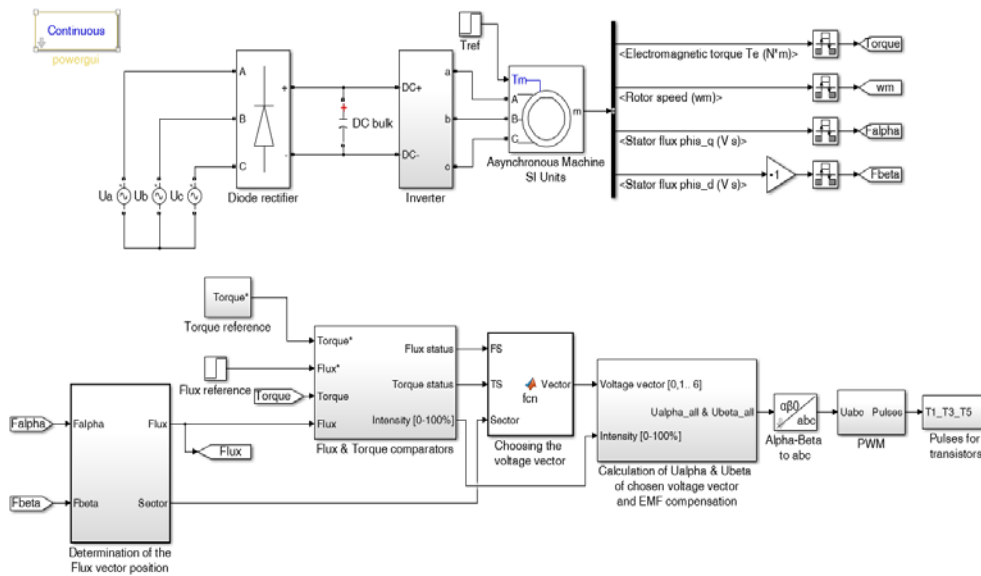


Figure 3. Main window of simulation model of DVI-DTC algorithm in Matlab/Simulink

Model of hardware (three-phase grid voltage supply, diode rectifier, DC bulk capacitor, inverter and Asynchronous machine) is made by using *Sim Power Systems* toolbox and is shown in the upper part of Fig. 3. At the output of mathematical model of the asynchronous machine automatically estimated values of torque, speed, α and β components of the stator flux are used and it is not necessary to make estimators for these quantities particularly. This simplification of the model can be justified by the fact that the estimation of motor quantities is not the topic of the paper. Besides, all estimators shown in [11], [12], [13] provide sufficiently accurate results given the adequate motor parameters. The influence of parameter deviation and measurement uncertainties was the topic of many papers [14], [15], with clear recommendations for application in real systems.

The proposed control algorithm is presented at the bottom of Fig. 3. The first subsystem (from left to right) calculates the magnitude and argument of the stator flux. Based on the argument of the flux, determination of sector (1 to 6, as presented in Fig. 1a) of the flux vector location is done.

The next subsystem shown in Fig. 3 contains two-level (classical) flux comparator and multilevel torque comparator. Inputs to the subsystem are torque and flux references and estimated torque and flux values. Flux and torque comparators are presented in Fig. 4a. Input to the flux comparator is the flux error and inputs to the multilevel torque comparator are torque error, specified number of used different voltage intensities (k) and comparator limits (in this specific case for $k=6$ voltage vectors torque comparator limits are set from $T_{bw}(1)$ to $T_{bw}(6)$). The initial script file (M-file) automatically determines limits of torque comparator for desired number of voltage intensities before starting the simulation. The M-file allows the user to choose different number of voltage vector intensities ($k=1\dots6$) as shown in Fig. 1a (case of three voltage vector intensities). Output of the flux comparator (*Flux status*) may either be 0 (demand to reduce) or 1 (demand to increase the flux). Outputs of torque

comparator are intensity of the applied voltage vector and the *Torque status*. In the case of using 4 different voltage intensities, algorithm chooses 25%, 50%, 75% or 100% of the selected voltage vector and *Torque status* which takes values of -1 (demand to reduce), 0 (to hold) or 1 (to increase the torque).

Based on the flux and the torque status, and the sector where stator flux vector is located, the appropriate voltage vector is chosen and it is presented with function block in Fig. 3.

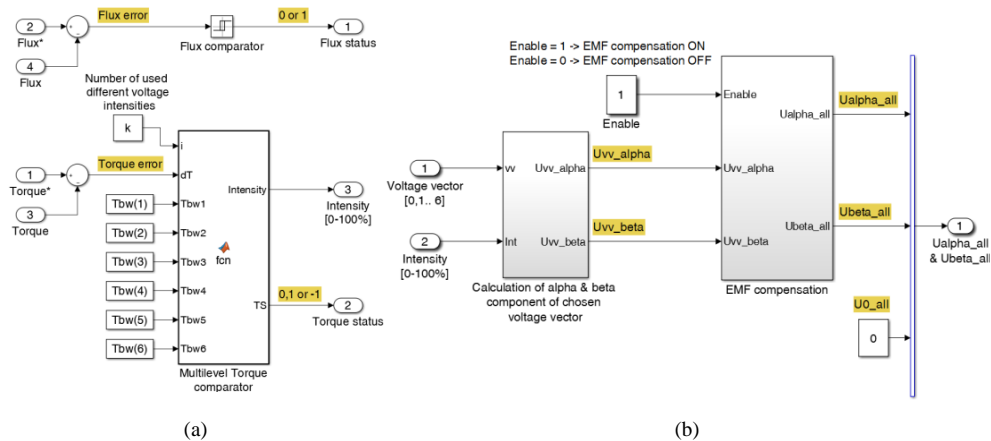


Figure 4. Subsystem Flux & Torque comparators (a) and subsystem Calculation of U_{α} & U_{β} of chosen voltage vector and EMF compensation (b)

The next subsystem presented in Fig. 3 is *Calculation of U_{α} & U_{β} of chosen voltage vector and EMF compensation*. The interior of this subsystem is presented in Fig. 4b. It contains two subsystems (*Calculation of alpha & beta component of chosen voltage vector* (left) and *EMF compensation* (right)).

The first subsystem calculates α and β component of chosen voltage vector (U_{vv_alpha} and U_{vv_beta}), as shown in Fig. 5. If the voltage vector is not zero voltage the switches (*Switch 1* and *Switch 2*) pass through upper inputs (U_{vv_alpha} and U_{vv_beta}) respectively, but if voltage vector is zero the switches pass through bottom inputs ($U0_alpha=0$, $U_{vv_beta}=0$).

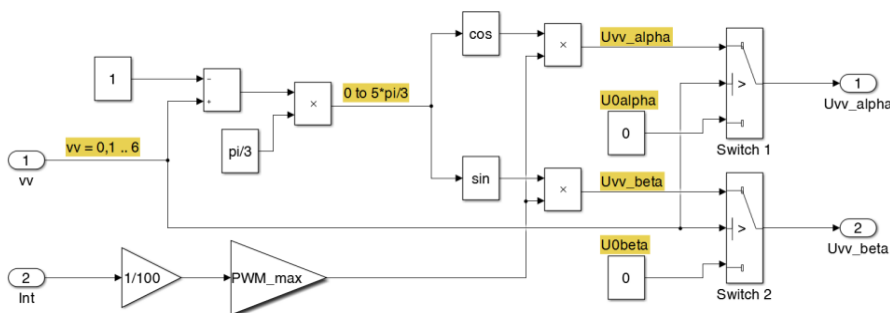


Figure 5. Subsystem Calculation of α & β component of chosen voltage vector

The EMF compensation is presented in Fig. 6. Inputs of the subsystem are previously calculated α and β components of chosen voltage vector (U_{vv_alpha} and U_{vv_beta}), estimated α and β components of the stator flux vector (F_{alpha} and F_{beta}) and angular frequency (ω_m) – motor speed. Results of multiplying α and β components of the stator flux with angular frequency are subtracted/summed with previously calculated α and β voltage components as it is presented in Fig. 6. This way α and β voltage components (U_{alpha_all} and U_{beta_all}) of resulting voltage vector (Fig. 1b) are determined. If the magnitude of resulting voltage vector is greater than allowed maximum value (PWM_max), switches 3 and 4 pass the upper inputs ($U_{alpha_max} = PWM_max \cdot \cos(\arg(U))$ and $U_{beta_max} = PWM_max \cdot \sin(\arg(U))$), otherwise pass U_{alpha_all} and U_{beta_all} . This subsystem also contains logical input (*Enable*) that enables the EMF compensation (switches 5 and 6 pass a new calculated α and β components of voltage vector that should be applied when the *Enable* is logically high, otherwise the EMF compensation is not in use).

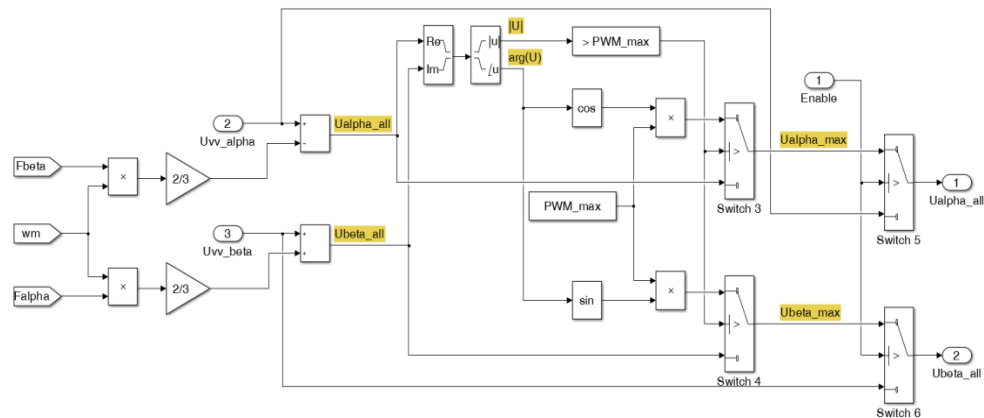


Figure 6. Subsystem EMF compensation

After determination of α and β components of voltage vector that should be applied it is needed to convert them to three phase *abc* system and to modulate with PWM, as presented in Fig. 7. The PWM subsystem also contains part responsible for magnetization of the machine. Magnetization is realized with active vector U_1 (inverter transistor T1 is switching with 20% duty cycle and transistors T3 and T5 are off; the states of T2, T4 and T6 transistors are the inverted states of T1, T3 and T5 respectively) until stator flux reaches its reference.

When the estimated flux reaches its specified reference value, *Switch 7* passes the upper input (PWM pulses to the inverter transistors).

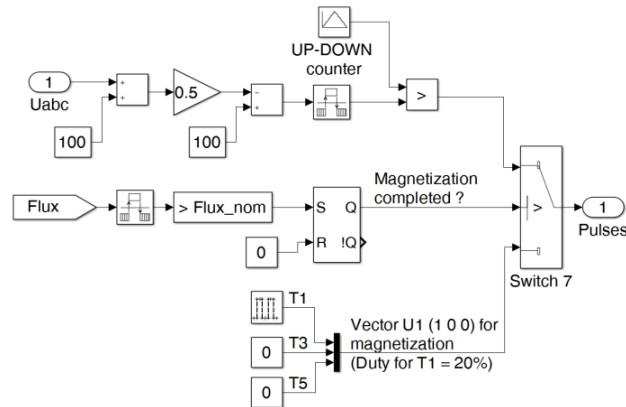


Figure 7. Subsystem PWM

To confirm efficiency of DVI-DTC algorithm in torque ripple reduction, simulations are done with not loaded motor for the case of only 3 different active voltage intensities. Torque reference is set to ± 0.3 p.u. (± 0.387 Nm) with cyclic change every 0.12s. The EMF influence is not compensated. The results of simulations are presented in Fig. 8. Fig. 8a shows estimated torque, torque reference and the corresponding comparator limits. Fig. 8b presents estimated stator flux and its α and β components. The motor speed is presented in Fig. 8c and α and β components of stator currents are shown in Fig. 8d. Nevertheless, Fig. 8a shows significant EMF impact to the torque resulting in deviation of torque from its reference at high speed.

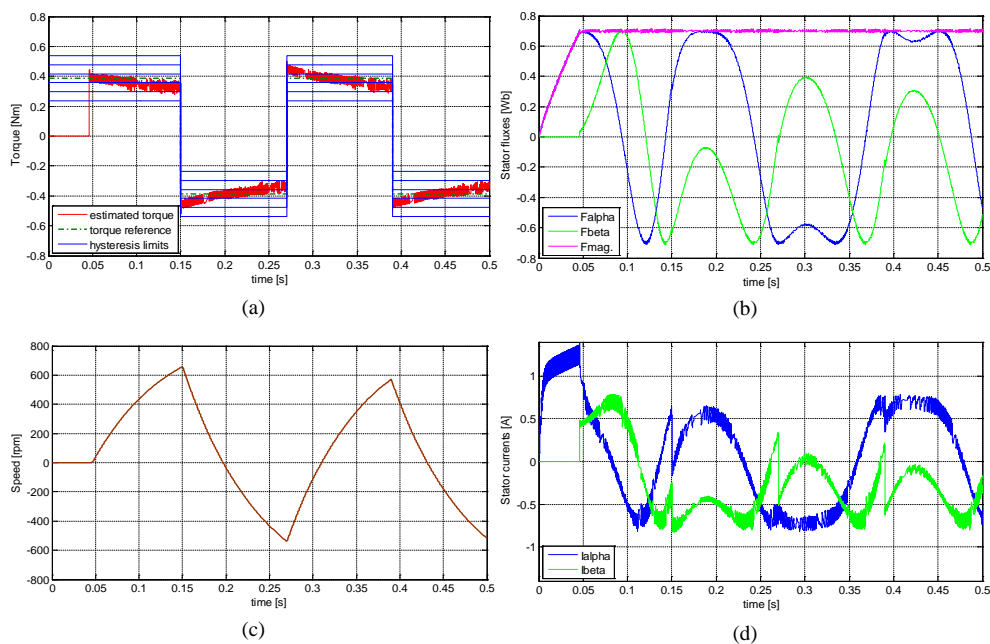


Figure 8. Estimated torque (a), stator flux (b), speed (c) and stator currents (d), for proposed DVI-DTC algorithm for 3 voltage intensities without EMF compensation

In order to present torque ripple reduction, as well as much better response of the torque in the case when EMF compensation is included, the DVI-DTC is tested with 4, 5 and 6 voltage vector intensities with and without EMF compensation. The results are presented in Fig. 9. The results show significant torque ripple reduction as a number of available voltage vector rises.

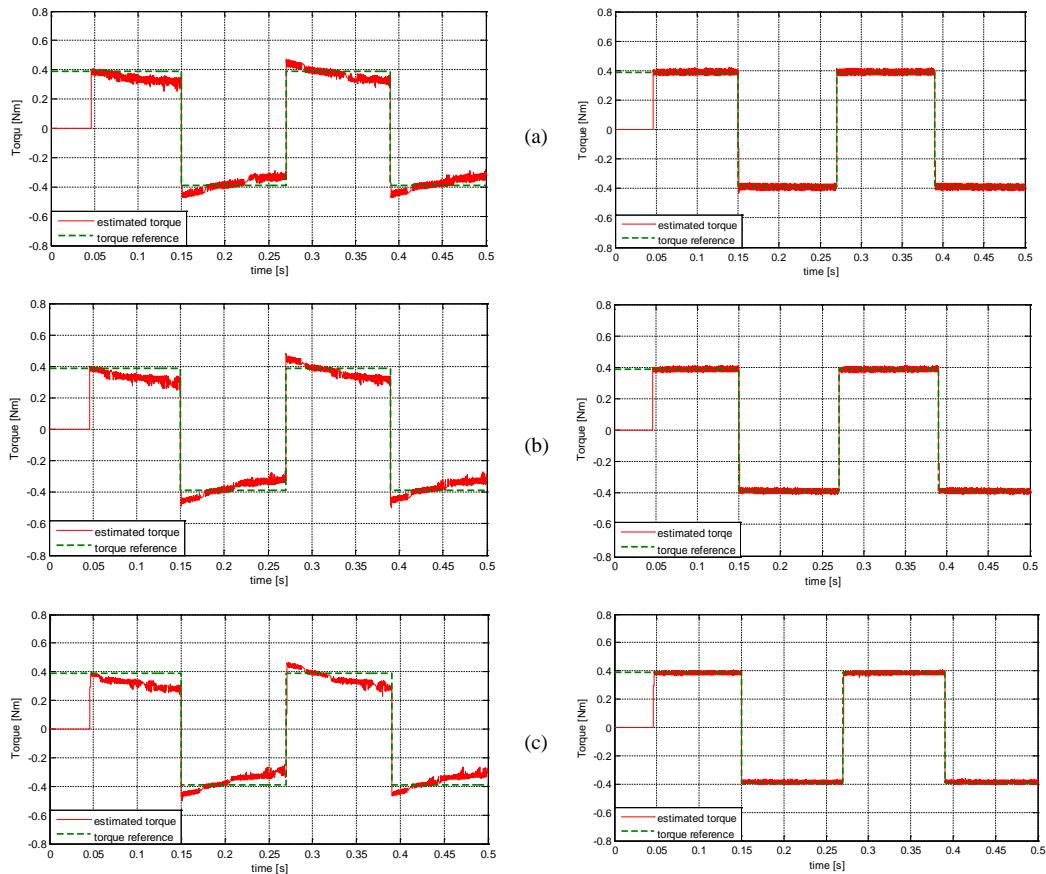


Figure 9. Torque response with 4 (a), 5 (b) and 6 (c) voltage vector intensities (simulation results) without compensated EMF (left) and with compensated EMF (right)

4. EXPERIMENTAL RESULTS

Proposed DVI-DTC algorithm is implemented and tested on Technosoft MSK2812 DSP platform combining ACPM 750W power module and TMS320F2812 processor. Detailed description of experimental setup and experimental results with reduced torque ripple related to different number of defined voltage vector intensities can be found in [6].

Experimental results obtained under the same conditions as in the simulations are presented in Fig. 10. The detailed description of flux and torque estimator is given in [16].

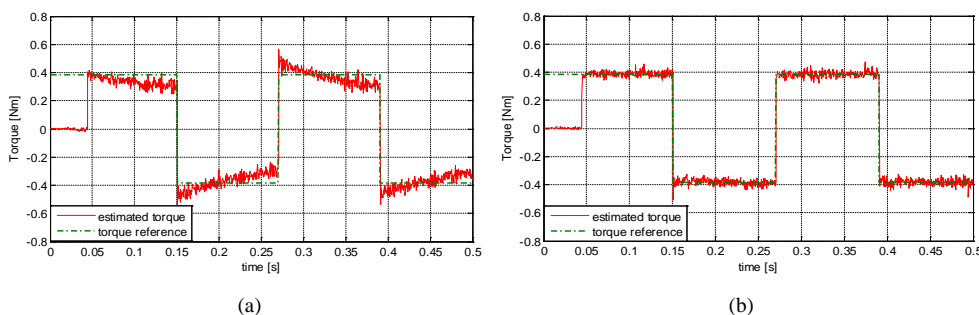


Figure 10. Torque response with 5 voltage vector intensities (experimental results) without compensated EMF (a) and with compensated EMF (b)

The experimental results show good consistency with the results of simulation as well as significant torque ripple reduction by increasing the number of different active voltage intensities.

5. CONCLUSION

This paper presents the simulation model of DVI-DTC control method using multiple discretized voltage vector intensities. The theoretical background of conventional DTC and DVI-DTC is presented at the beginning of the paper. Based on the theoretical background, simulation model and the most important simulation results were further presented. Results show significant torque ripple reduction with DVI-DTC method as number of defined discretized voltage intensities increases. Presented experimental results obtained on real DSP platform confirm simulation results. This design approach by developing and testing the control system by means of simulation before experimental verification provides better overview and understanding of the whole system. Simulation model allows us to test DTC control algorithm in different working conditions and to predict system behavior in critical operating points. This is extremely important in the process of predicting potential problems and obtaining their solutions during the development. Also, development and testing the DTC algorithm in simulating conditions allows students to better understand principles of DTC whilst exploring courses of electric drive control. Furthermore, these kind of simulations in engineering provide safe space for improvement and testing of control algorithms before practical implementation in real DSP systems.

ACKNOWLEDGEMENTS

This work was supported by grants (Projects No.TR33016 and TR33024) from the Ministry of Education, Science and Technological Development of Serbia.

REFERENCES

- [1] D. Casadei, G. Serra, and A. Tani, "Improvement of direct torque control performance by using a discrete SVM technique," *PESC 98 Rec. 29th Annu. IEEE Power Electron. Spec. Conf. (Cat. No.98CH36196)*, vol. 2, pp. 997–1003, 1998.
- [2] D. Casadei, G. Serra, and K. Tani, "Implementation of a direct control algorithm for induction motors based on discrete space vector modulation," *IEEE Trans. Power Electron.*, vol. 15, no. 4, pp. 769–777, 2000.

- [3] F. Betin, G. A. Capolino, D. Casadei, B. Kawkabani, R. I. Bojoi, L. Harnefors, E. Levi, L. Parsa, and B. Fahimi, "Trends in electrical machines control: Samples for classical, sensorless, and fault-tolerant techniques," *IEEE Ind. Electron. Mag.*, vol. 8, no. 2, pp. 43–55, 2014.
- [4] A. Damiano, G. Gatto, I. Marongiu, and A. Perfetto, "An improved multilevel DTC drive," in *PESC Record - IEEE Annual Power Electronics Specialists Conference*, 2001, vol. 3, no. 2, pp. 1452–1457.
- [5] L. Zheng, J. E. Fletcher, B. W. Williams, and X. He, "A novel direct torque control scheme for a sensorless five-phase induction motor drive," *IEEE Trans. Ind. Electron.*, vol. 58, no. 2, pp. 503–513, 2011.
- [6] M. Rosic and M. Bebic, "Analysis of Torque Ripple Reduction in Induction Motor DTC Drive with Multiple Voltage Vectors," *Adv. Electr. Comput. Eng.*, vol. 15, no. 1, pp. 105–114, 2015.
- [7] I. Takahashi and T. Noguchi, "A New Quick-Response and High-Efficiency Control Strategy of an Induction Motor," *IEEE Trans. Ind. Appl.*, vol. IA-22, no. 5, pp. 820–827, Sep. 1986.
- [8] M. Rosić, M. Bebić, and N. Đorđević, "Torque Ripple Reduction in DTC with Discretized Voltage Intensities," in *18th International Symposium on POWER ELECTRONICS - EE2015*, 2015, pp. 1–6.
- [9] M. Rosić, M. Bjekić, and M. Božić, "Modeling of Direct Torque Control with discrete voltage vectors in simulink," in *Proc. 56th ETRAN Conference, Zlatibor, June 11-14, 2012*, 2012, p. EE2.3. 1–4.
- [10] M. Rosic, A. Lazic, and M. Bozic, "Graphical user interface for comparison of Direct Torque Control characteristics of Induction Motor with discrete and continuous voltage vectors," in *5th International Conference TECHNICS AND INFORMATICS IN EDUCATION TIO 2014, Faculty of Technical Sciences Čačak, 30–31th May 2014*, 2014, no. May, pp. 175–181.
- [11] J. Hu and B. Wu, "New integration algorithms for estimating motor flux over a wide speed range," *IEEE Trans. Power Electron.*, vol. 13, no. 5, pp. 969–977, 1998.
- [12] J. Holtz and J. Quan, "Sensorless vector control of induction motors at very low speed using a nonlinear inverter model and parameter identification," *IEEE Trans. Ind. Appl.*, vol. 38, no. 4, pp. 1087–1095, Jul. 2002.
- [13] A. W. F. Silveira, D. A. Andrade, C. A. Bissochi, T. S. Tavares, and L. C. S. Gomes, "A Comparative Study Between Tree Philosophies of Stator Flux Estimation for Induction Motor Drive," *2007 IEEE Int. Electr. Mach. Drives Conf.*, vol. 2, no. 1, pp. 1171–1176, May 2007.
- [14] P. L. Jansen and R. D. Lorenz, "A Physically Insightful Approach to the Design and Accuracy Assessment of Flux Observers for Field Oriented Induction Machine Drives," *IEEE Trans. Ind. Appl.*, vol. 30, no. 1, pp. 101–110, 1994.
- [15] B. E. Heinbokel and R. D. Lorenz, "Robustness Evaluation of Deadbeat, Direct Torque and Flux Control for Induction Machine Drives Induction Machine Model and DB-DTFC," in *EPE '09. 13th European Conference on Power Electronics and Applications, 2009*, 2009, pp. 1–10.
- [16] M. Rosic, "Ripple reduction in Direct Torque Control of induction motor by using multilevel comparators," - doctoral dissertation, University of Belgrade, Faculty of Electrical Engineering, 2016.